Naunyn-Schmiedeberg's Arch Pharmacol (2001) 364 : 397–408
DOI 10.1007/s002100100462

ORIGINAL ARTICLE

S. Dhein · S.-B. Hammerath

Aspects of the intercellular communication in aged hearts: effects of the gap junction uncoupler palmitoleic acid

Received: 7 March 2001 / Accepted: 11 June 2001 / Published online: 23 August 2001

Abstract Although cardiac arrhythmia is among the most common causes of death and the percentage of aged people in our population is steadily increasing, only little is known on age-dependent changes in intercellular coupling, anisotropy and electrophysiology in mammalian heart. Thus, we wanted to investigate electrophysiology and anisotropy in aged vs. young rabbit heart, as well as the response to the gap junction uncoupler palmitoleic acid.

Spontaneously beating hearts of young mature (6±1 months, *n*=14) and aged (32±5 months, *n*=9) male White New Zealand rabbits (Langendorff technique) were submitted to epicardial 256-channel potential mapping. Cumulative concentration-response curves for palmitoleic acid (0.2–20.0 μM) were carried out. At certain time points anisotropy was measured by application of rectangular pulses and the determination of longitudinal and transversal conduction velocity. Finally, hearts were processed histologically for Van Gieson staining or connexin43 immunostaining.

In spontaneously beating aged hearts we found enhanced dispersion of activation-recovery intervals (15.9±1.6 ms vs. 10.8±2.0 ms, $P<0.05$), prolonged (31.2±1.4 ms vs. 25.2±1.8 ms, $P<0.05$) and fractionated QRS complexes. We found reduced transversal velocity (0.22±0.01 m/s vs. 0.27±0.02 m/s, $P<0.05$) and enhanced anisotropy (2.6± 0.2 vs. 2.0±0.1, $P<0.05$) in aged hearts, while longitudinal velocity was not changed. Histologically, in ventricles from aged hearts we found diffuse deposition of collagen lateral to the fibers and more pronounced expression of connexin43 at lateral cell borders. The functional changes in ventricles from aged hearts were mimicked by application of palmitoleic acid to young hearts in a concentration-dependent manner. In aged hearts this concentration-response curve started at higher initial values, but finally reached similar maximum values.

In aged hearts ventricular intercellular coupling transverse to the fiber axis is reduced. Correlates are increased dispersion, slowed transverse conduction and increased anisotropy, and enhanced Cx43 immunostaining at the lateral cell borders. The functional age-dependent changes can be mimicked in young hearts by the gap junction uncoupler palmitoleic acid.

Keywords Age · Aging · Anisotropy · Gap junction · Connexin · Heart · Cx43

S. Dhein (✉) · S.-B. Hammerath
Institute of Pharmacology, University of Halle,
Magdeburger Strasse 4, 06097 Halle (Saale), Germany
e-mail: stefan.dhein@medizin.uni-halle.de,
Tel.: +49-345-5574420, Fax: +49-345-5571835

Introduction

Cardiac arrhythmias are a major cause of death, particularly in the elderly population. Although it is well known that cardiac histology changes with growing age by increasing deposition of collagen and fat (Klausner and Schwartz 1985), which influences the electrophysiological properties (Gottwald et al. 1997), only little is known whether these changes also lead to alterations of the intercellular communication. One could imagine that increased deposition of collagen may result in reduced communication, which might in turn lead to a change in anisotropy as shown in the atrium (Spach and Dolber 1986). However, it is unclear whether a similar situation occurs in the ventricles. In addition, it is unclear whether the pattern of distribution of connexin 43 (Cx43), which is the most important gap junctional protein in the ventricle (for review see Dhein 1998a, 1998b), might be changed.

Thus, we wanted to investigate whether (a) the Cx43 distribution might be altered with increasing age or (b) – as a functional parameter – the anisotropy of the ventricle may change with age. The key finding we show here for the first time is that aging leads to biophysical changes in the ventricle with enhanced anisotropy due to reduced transversal action potential conduction velocity while longitudinal velocity was nearly unchanged. The reduction in transversal conduction velocity was in parallel to enhanced collagen deposition lateral to the fibers and increased Cx43 immunostaining at the lateral cell borders, although

the cells were separated by strands of collagenous tissue. The functional correlate was the reduced transversal velocity and a change in the QRS complex with broadened and fractionated QRS complexes. These findings suggested that aging may lead to impaired intercellular communication especially in transverse direction. Thus, we wanted to investigate whether (c) the gap junction uncoupling agent palmitoleic acid (Burt et al. 1991; Dhein et al. 1999), a naturally occurring unsaturated C_{16} fatty acid, applied to young hearts may mimic the changes observed in aged hearts. As a model we decided to investigate isolated hearts from rabbits of different age (young mature at 6 months vs. aged at 32 months). This model has been established previously (Gottwald et al. 1997). Indeed, application of palmitoleic acid led to the same functional changes as observed in ventricles of aged hearts.

Materials and methods

All experiments were performed in accordance with the ethical rules of the Council for International Organization of Medical Science and the German laws for animal welfare. Two groups of male White New Zealand rabbits have been investigated: young mature rabbits (6±1 months, *n*=17) and old rabbits (32±5 months, *n*=12; conventional, normally fed ad libitum; Rollie, Langenhagen, Germany). Body weight was 2436±60 g (young) and 4465±175 g (aged). Heart wet weight was 8±0.3 g (young) and 22±2 g (aged).

Mapping experiments in isolated hearts. The method of heart preparation and epicardial potential mapping has been described in more detail previously (Dhein et al. 1993) and will be explained only briefly in the following paragraph. Male White New Zealand rabbits were treated with 1000 IU/kg heparin i.v. 5 min before they were stunned by a sharp blow on the neck and killed rapidly by subsequent exsanguination as approved by the local committee for animal care. The heart was excised, prepared and perfused according to the Langendorff technique at constant pressure (70 cmH_2O) with modified Tyrode's solution of the following composition: Na^+ 161.02, K^+ 5.36, Ca^{2+} 1.8, Mg^{2+} 1.05, Cl^- 147.86, HCO_3^- 23.8, PO_4^{2-} 0.42 and glucose 11.1 mmol/l, equilibrated with 95% O_2 and 5% CO_2 (pH=7.4). The surface temperature of the heart was 37°C. The hearts were connected to a 256-channel mapping system HAL3 (ELSA, Aachen, Germany; temporal resolution: 4 kHz/channel; amplitude resolution: 0.04 mV, interchannel coupling < –60 dB; bandwidth of the system: 0.5 Hz–20 kHz) as described previously (Dhein et al. 1988). A total of 256 AgCl electrodes were cast in four polyester plates (in 8×8 orthogonal matrices with 1-mm interelectrode distance) which were attached to the heart surface in an elastic manner, so that they could follow the heart movements easily without dislocation. The hearts were beating at their spontaneous rate during the experiment. After 45 min of equilibration, we administered palmitoleic acid, an unsaturated C_{16} fatty acid known as a gap junction uncoupling agent (Burt et al. 1991; Dhein et al. 1999), in cumulative concentrations of 0.2, 1, 2, 5, 10 and 20 μM, each concentration being applied for a period of 15 min. Palmitoleic acid (stock solution dissolved in Tyrode solution) was infused intracoronarily at a rate of 1 ml/min using a Perfusor VI (Braun, Melsungen) with short plastic tubing. Epicardial potential mapping was performed in each experimental phase during periods of constant cycle length of at least 4 min, in order to make it possible to compare the activation patterns (of single heart beats) or their alterations. In addition, the functional parameters maximum systolic left ventricular pressure (LVP) and coronary flow (CF) were assessed continuously as described (Dhein et al. 1993). The delay between the end of the *P*-wave and the first normal ventricular activation was assessed as *PQ*-time as a measure for the atrioventricular conduction time.

Further analysis of the 256 unipolar electrograms included assessment of the amplitude of the QRS complexes as the peak-to-peak amplitude (PTP; mV), which is known to be an indirect indicator of the velocity of the travelling activation wave in the tissue beneath the electrode (Spach and Dolber 1986). In addition, the duration of the QRS complex in the epicardial electrograms was determined. Moreover, the activation time points at each electrode were determined as $t(dU/dt_{min}$; Dhein et al. 1993; Durrer and Van der Tweel 1954), and the repolarization time points as $t(dU/dt_{max})$ during the *T*-wave as described (Dhein et al. 1993; Millar et al. 1985). After automatic determination activation and repolarization time points were verified (or corrected if necessary) manually by the experimentator. From these data for each electrode an activation-recovery interval (ARI, indicating epicardial potential duration) was calculated. The corresponding distribution of ARI was analyzed for each area of the heart (i.e. front, left, right or back wall) calculating the standard deviation of ARI at 64 electrodes and expressed as ARI dispersion [i.e. standard deviation (SD) of ARI at 256 electrodes]. In addition, QTc was calculated according to Bazett's equation (Bazett 1920), i.e. $QTc=QT\times\sqrt{(HR/60)}$. From the activation time points an activation sequence was determined. From this sequence, the total activation time (TAT; ms) was assessed as the delay between activation of the first and activation of the last of the 256 electrodes. The spreading of epicardial excitation was analyzed using a vector transformation (Dhein et al. 1993). In order to allow a quantitative and comparative description of the activation process, for each electrode an activation vector was calculated from the activation times and the locations of the surrounding electrodes which were activated after the central electrode (i.e. a maximum number of eight), as described by Dhein et al. (1990) and Müller et al. (1991). These vectors give direction and apparent velocity of local activation. The percentage of similar vectors (VEC) between heart beats in the various experimental phases compared with those under control conditions was determined (vectors deviating not more than 5° from their original direction were considered to be similar). The critical value beneath which arrhythmia often occurs (see above) for VEC similarity is 10% as determined in previous studies (Dhein et al. 1988, 1993). Thus, VEC characterizes the geometry of the epicardial activation process, and represents the beat similarity of the cardiac impulse as compared to heart beats under control conditions. Thus, decreasing values of VEC indicate progressive deviation from the initial (control) activation pattern.

Assessment of anisotropy, transverse and longitudinal velocity. In order to determine transverse and longitudinal conduction velocities and their ratio, i.e. the anisotropy, at certain time points (after 40-min equilibration and after 15 min of 20 μM palmitoleic acid), a single brief rectangular pulse (bipolar electrode, 1 ms duration and double threshold) was applied at the back ventricular wall and the isochrones of activation were determined as described (Dhein et al. 1999). From the isochrones and the fiber orientation of the ventricle the longitudinal (V_L) and transversal conduction velocity (V_T) were calculated as described (Dhein et al. 1999). Anisotropic ratio was determined as V_L/V_T. As an indicator of local velocity the time interval (in ms) between the beginning of the QRS complex and the activation time point (b_{QRS}-ACT; Burgess et al. 1988) was determined at electrodes in areas with transverse and in areas with longitudinal conduction.

Measurement of cell capacitance. In additional experiments (*n*=3 young and *n*=3 aged hearts) we measured cell capacitance in isolated cells (*n*=60 cells for each group). Cells were isolated from perfused hearts using a standard collagenase method (Dhein 1998a). The isolated cells were patched (whole-cell configuration) using a SEC-05 patch clamp amplifier (npi-electronic, Tamm, Germany) at a switching frequency of 25–30 kHz, 10 kHz sampling rate, with two 2–3 MΩ glass-microelectrodes filled with: CsCl 125, NaCl 8, $CaCl_2$ 1, EGTA 10, Na_2ATP 2, MgATP 3, Na_2GTP 0.1, HEPES 10 mM, pH 7.2 with CsOH. Cells were superfused with Tyrode solution. Cell capacitance was determined for each cell prior to capacitance compensation from the capacitive current evoked by a –10 mV pulse (from a holding potential of –40 mV).

Immunohistological studies. At the end of the experiments, the hearts were frozen in liquid nitrogen and thereafter processed for classical histology (H&E staining or Van Gieson staining) or for immunohistochemical detection of Cx43 as described (Dhein 1998a). Indirect immunofluorescence was performed on 10-µM cryosections cut in parallel to the fiber longitudinal axis. The specimens were fixed with methanol (30 min, 4°C), blocked with phosphate-buffered bovine serum albumin (BSA) solution [20 min at room temperature (RT); composition: 8 g NaCl, 0.2 g KCl, 1.15 g Na_2HPO_4, 0.2 g KH_2PO_4, 1 g BSA in 1 l H_2O, pH 7.5], incubated with the primary anti-Cx43 antibody (MAB 3068; Chemicon, Temecula, Calif., USA) overnight (4°C) and subsequently exposed to FITC-labeled secondary antibody (Sigma, USA). Finally, the slides were thoroughly washed with phosphate-buffered saline and embedded in Karyon (Merck, Darmstadt, Germany).

The slides were investigated at ×1000 magnification using a commercial image analysis system (JAVA; Jandel Scientific, Erkrath, Germany) and a Zeiss Axiolab fluorescence microscope. For evaluation only cells which were cut longitudinally were analyzed: each cell was divided into four areas of equal size: the longitudinal cell axis was determined and divided into four sections of equal length giving four areas: the left and right cell pole and the two mid areas. We measured the length of the plasma membrane (LM) of each section and the length of the immunofluorescence-positive membrane (PLM) of the section, and calculated the ratio between positively stained membrane length and membrane length $PLM_{section}/LM_{section}$.

Six young and n=6 aged animals were investigated by immunostaining. Five slide preparations per specimen and about ten cells per slide were analyzed, i.e. 300 cells in each group.

Statistics. If not stated otherwise, all values are given as means ± SEM of n experiments. We used 14 young rabbits and 9 old rabbits for control and n=7 aged and n=7 young rabbits for the palmitoleic acid series. Experimental data were analyzed by computer-supported iterative non-linear regression analysis using InPlot program (GraphPad Software, San Diego, Calif., USA) and were fitted to sigmoid curves. Significance was analyzed by analysis of variance (ANOVA) for comparison of multiple groups. If ANOVA indicated significant differences, either Wilcoxon rank test for paired observations or Mann-*U*-test for unpaired observations were performed (Systat; Jandel, Erkrath, Germany). The level of significance was $P<0.05$.

Chemicals. All chemicals used in this study were of analytical grade. Palmitoleic acid was from Sigma (Deisenhofen, Germany) and was dissolved in 70% methanol yielding a 10^{-2} M stock solution; Cx43 monoclonal antibody was from Chemicon (Temecula, Calif., USA). The $F_{a,b}$-specific anti-mouse IgG FITC-labeled antibody was obtained from Sigma (Deisenhofen, Germany). All other chemicals were purchased from Merck (Dresden, Germany), except heparin which was from Serva (Heidelberg, Germany

Results

Basic electrophysiological findings

We found that the epicardial electrograms of aged hearts (n=9) were different from those of young hearts (n=14): the QRS complex was prolonged (young: 25.2±2 ms vs. aged: 31.2±1.4 ms, $P<0.05$) and fractionated. The amplitude of the QRS complex was slightly reduced in aged hearts (young: 3.7±0.4 mV vs. aged: 3±0.3 mV, P=0.045; Fig. 1). The total activation time (for all 256 electrodes, i.e. all four walls) was significantly prolonged in aged hearts (young: 11.9±0.7 ms vs. aged: 16.6±1.7 ms, $P<0.05$).

Atrioventricular conduction was slightly but not significantly prolonged in aged hearts as became evident from the *PQ*-interval (young: 45±3 ms vs. aged: 49±4 ms).

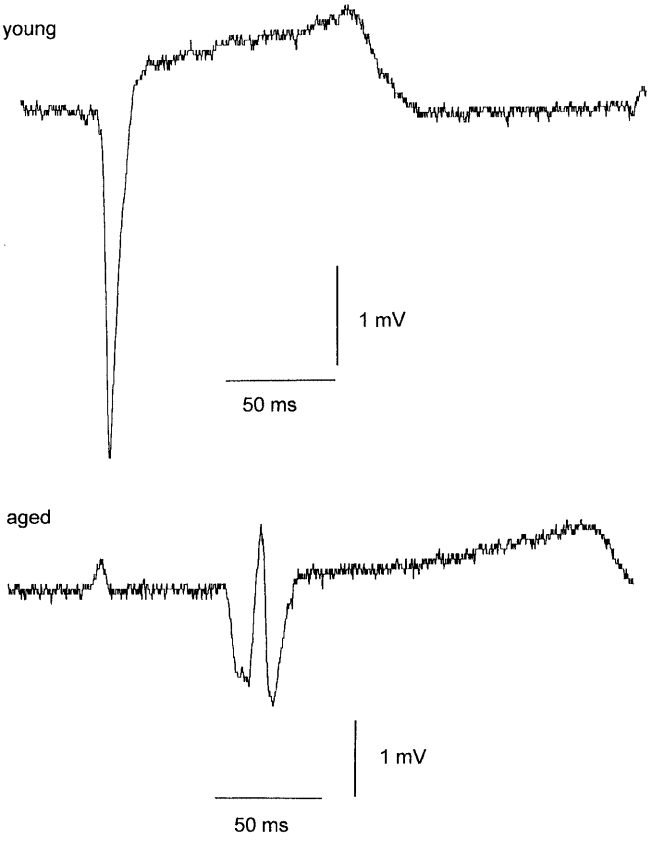

Fig. 1 Original epicardial potential registration from the front wall of a young rabbit heart (*upper panel*) and an aged heart (*lower panel*). Note the prolongation and the reduced amplitude of the QRS complex

Moreover, the mean activation-recovery interval (at all 256 sites) was slightly prolonged (young: 130±5 ms vs. aged: 139±9 ms, n.s.; but for more detailed and regional analysis see below). The basic cycle length was also slightly (n.s.) prolonged in aged hearts (young: 344±22 ms vs. aged: 414±42 ms, n.s.). Calculating QTc according to Bazett's correction revealed no significant prolongation of QTc in aged hearts if calculated for all 256 electrodes (young: 0.323±0.007 s vs. aged: 0.327±0.015 s, n.s.). If QTc was calculated separately for different regions, a prolongation at the back and right wall became evident (young: 0.213±0.007 s vs. aged: 0.410±0.017 s, $P<0.05$; and see below).

In addition, the dispersion of the activation-recovery intervals, i.e. the standard deviation of all 256 activation recovery intervals, was significantly enhanced (young: 10.8±2 ms vs. aged: 15.9±1.6 ms, $P<0.05$) indicating enhanced inhomogeneity of activation-recovery intervals (ARI; Fig. 2). Further analysis of this inhomogeneity revealed differences in the mean ARI between right wall and left wall (young: right: 136±7 ms; left: 124±5 ms; aged: right: 147±9 ms; left: 133±9 ms) and between front and back wall in both young and aged hearts (young: front: 137±5 ms; back: 125±6 ms; aged: front: 132±9 ms; back: 143±9 ms; Fig. 2). Thus, in aged hearts mean ARI

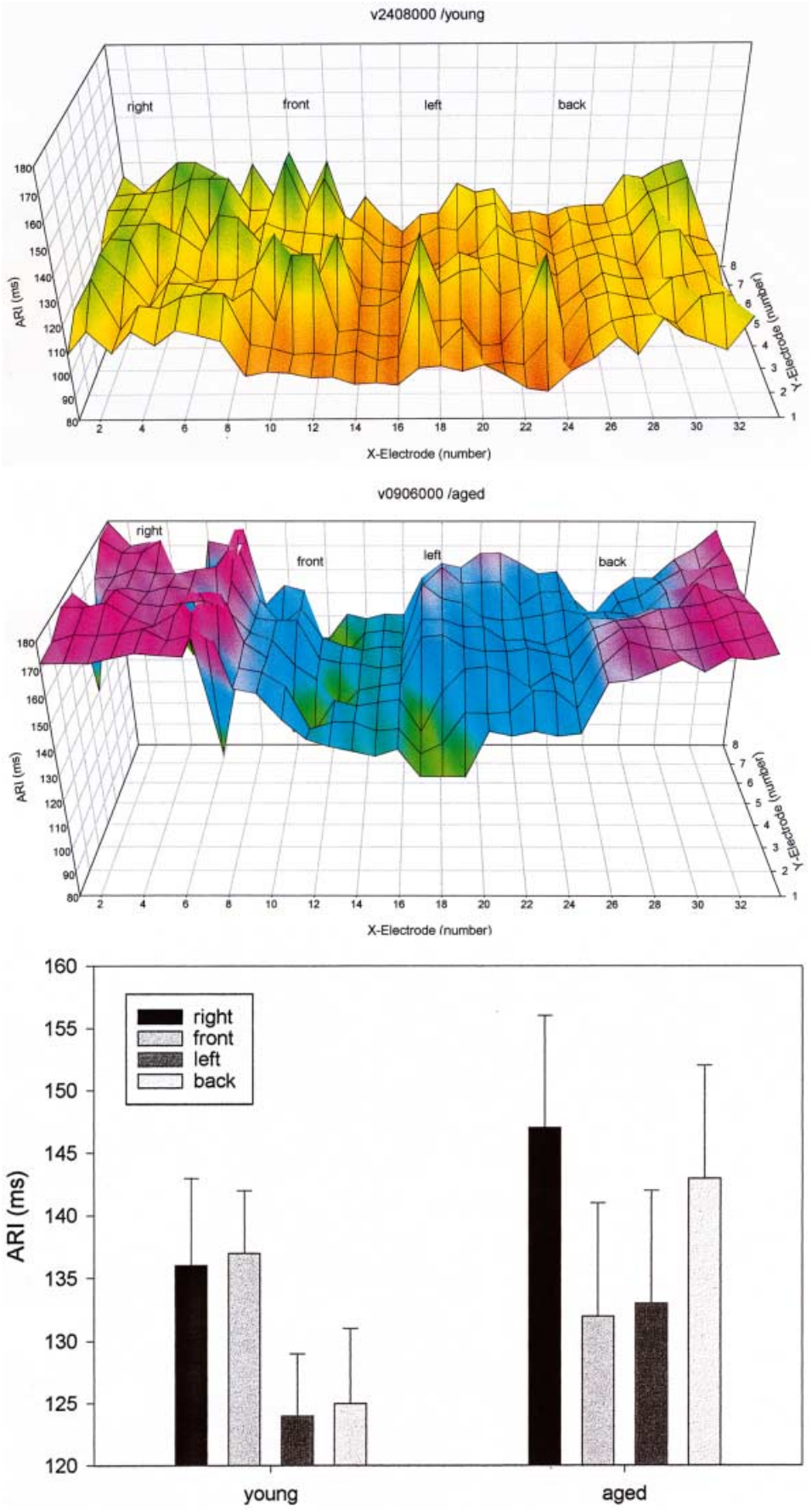

Fig. 2 Original registration of the distribution of the epicardial activation-recovery intervals on the cardiac surface in a young (*upper panel*) and aged heart (*middle panel*) measured at 256 electrodes on the ventricular surface. The spacing between the electrodes was 1 mm. Note the higher inhomogeneity, and thus higher dispersion, in the aged heart. The *lower panel* shows the mean activation-recovery interval ± SEM for the right, front, left and back wall in young (n=7) and aged hearts (n=7)

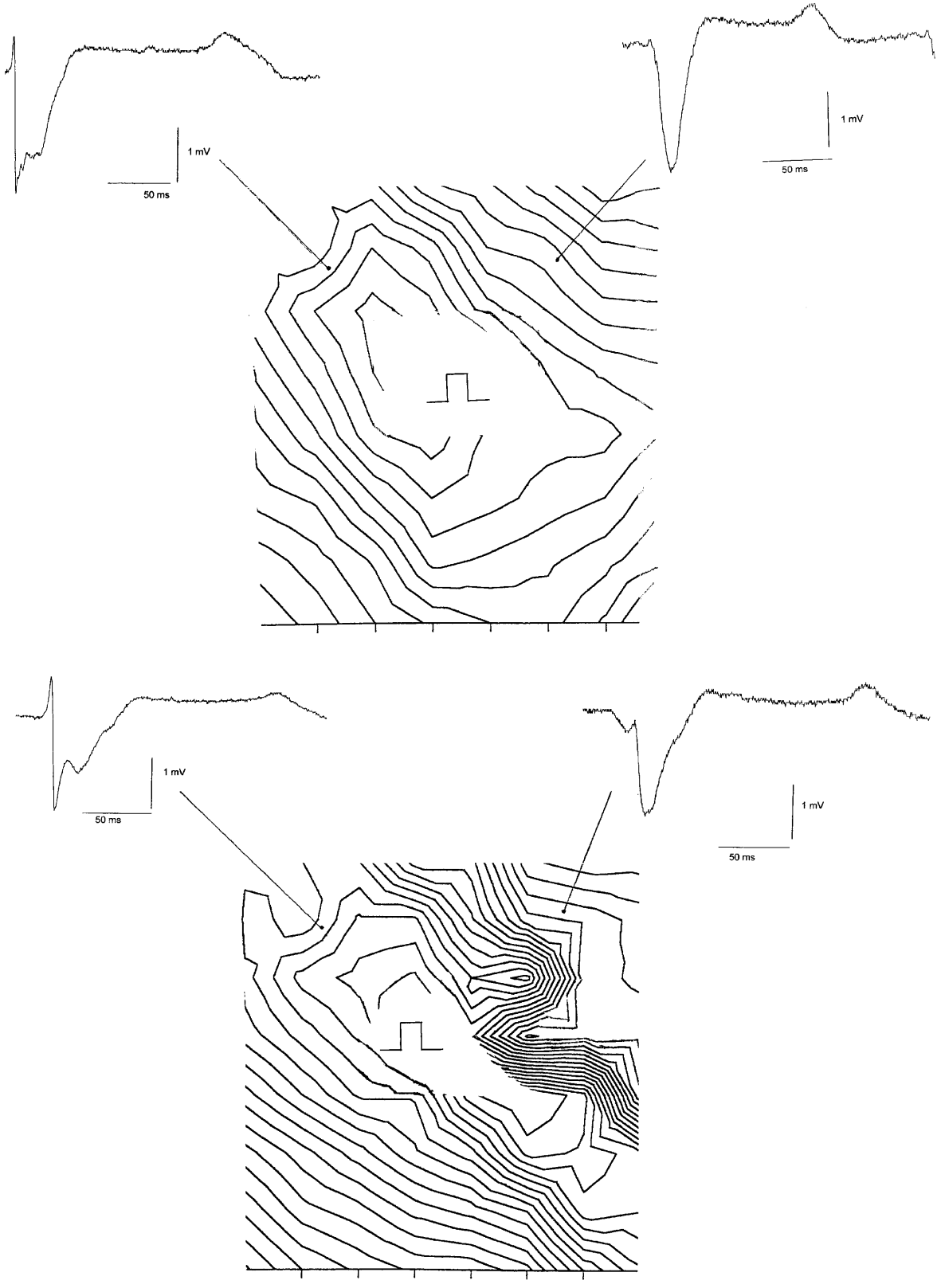

Fig. 3 Isochrones of the epicardial activation after application of an external stimulus at the back wall of a young (*upper panel*) and an aged heart (*lower panel*). The isochrones represent 1.25 ms, i.e. the area which is activated within these 1.25 ms. The interelectrode distance was 1 mm; the ticks at the lower axis indicate 1 mm distance. For each heart a typical extracellular potential recording in longitudinal and transversal direction is given. Note the elongated elliptical form and the non-uniformities of the isochrones in the aged heart. From the depicted unipolar electrograms it can be seen that the time interval between beginning of the QRS complex and the fastest negative intrinsic deflection (= activation time point) is longer in areas with transverse conduction (see also Table 1)

was slightly prolonged at the right (147±9 ms) and back (143±9 ms) wall if compared with young hearts (136±7 ms, right, and 125±6 ms, back; P=0.048).

Regarding the activation pattern, the percentage of activation vectors with a similar direction was significantly lower in aged hearts (young: 38.8±3.2% vs. aged: 29.8± 5.7%, P<0.05) for two succeeding heart beats, i.e. the beat-to-beat variability of the activation pattern was enhanced.

The developed left ventricular pressure was somewhat reduced in aged hearts (young: 98.9±7.2 mmHg vs. aged: 84.7±3.1 mmHg, P<0.05), while the coronary flow was a little higher in these hearts (young: 41.8±1.9 ml/min vs. 48.4±2.6 ml/min, n.s.).

Anisotropy, conduction velocities

Application of rectangular pulses delivered at a single site led to an activation spreading with elliptical isochrones as can be seen from Fig. 3. These ellipses appeared to be somewhat elongated in aged hearts. Detailed analysis of the velocities longitudinal and transverse to the fibers revealed that in aged hearts the transverse conduction velocity was significantly reduced by 25±8% as compared to young hearts (young: 0.27±0.02 m/s vs. aged: 0.22±0.01 m/s, P<0.05), while the longitudinal conduction velocity was not significantly altered (reduction by –2±2%; young: 0.57± 0.02 m/s vs. aged: 0.55±0.05 m/s, n.s.). Thus, the anisotropic ratio, V_L/V_T, was enhanced (young: 2.03±0.1 vs. aged: 2.6±0.2, P<0.05). Moreover, it can be seen from Fig. 3 that the spreading of activation is more inhomogeneous in aged hearts and is accompanied by broader QRS complexes. Detailed analysis revealed that in areas of transverse propagation the time interval from the beginning of the QRS complex until the activation time point at that electrode (b_{QRS}-ACT) was generally more prolonged than in areas of longitudinal propagation. Moreover, while in areas with longitudinal conduction there was no difference (regarding this time interval) between aged and young hearts, in areas of transverse conduction this interval was significantly longer in aged than in young hearts (see Table 1). In addition, in aged hearts the isochrones were generally less uniform than in young hearts as can also be seen in an example in Fig. 3. As can be seen from Table 1, ARI was slightly longer in areas of longitudinal conduction if compared with areas of transverse conduction.

Effects of palmitoleic acid

As stated above, in aged hearts total activation time and QRS duration were prolonged, dispersion was enhanced and the percentage of activation vectors with a similar direction was reduced. Application of palmitoelic acid to young hearts mimicked these changes (Fig. 4). Concentration-response curves for these parameters ended up at the same maximum effects. Thus, application of palmitoleic acid concentration-dependently led to an increase in dispersion of ARI in both young (from 8.2±0.5 ms to 21.5± 0.8 ms) and aged hearts (from 12.8±1 ms to 21.6±1.5 ms). In aged hearts the basal dispersion of ARI was enhanced (see above), and at the highest concentration similar maximum values for dispersion were registered (Fig. 4A). As can be seen from Fig. 4, EC_{50} values were similar in both groups.

The mean total activation time (over all 256 electrodes) was also concentration-dependently prolonged by palmitoleic acid in young (from 11.9±0.7 ms to 15.2±1.8 ms) and aged hearts (from 16.6±1.7 ms to 18.0±1.3 ms) thus reaching similar maximum values at the maximum concentration. However, in aged ventricles the initial basal values for total activation time were significantly higher. Similar findings were obtained if the parts (right, front, left, back wall) of the ventricles were analyzed separately. Thus, at the right ventricle TAT (right) was initially 6.7± 0.8 ms (young) or 9.6±1.2 ms (aged) and was prolonged in presence of palmitoleic acid to a maximum of 10.5±1 ms (young) and 10.3±1 ms (aged; see Fig. 4B). EC_{50} values were similar.

In addition, a prolongation of the duration of the QRS complex was seen under the influence of increasing concentrations of palmitoleic acid reaching similar maximum values in both groups although starting at a higher basal value in aged hearts (Fig. 4C). Both curves showed similar EC_{50} values.

Regarding ventricular activation pattern, palmitoleic acid reduced significantly the percentage of vectors with similar direction (if heart beats in presence of palmitoleic acid were compared to previous heart beats under control conditions) in both young and aged hearts (Fig. 4D). As can be seen from the figure, already at the lowest concentration there was a high effect in both groups close to the maximum effect reached at the highest concentration.

Furthermore, we found a palmitoleic acid-induced concentration-dependent first degree atrioventricular block

Table 1 Time interval between beginning of the QRS complex and the activation time point (b_{QRS}-ACT interval; ms) and ARI (ms) at electrodes in areas with transverse and areas with longitudinal conduction in aged and young hearts

	Young	Aged	Young + palmitoleic acid (20 μM)
b_{QRS}-ACT interval in area with longitudinal conduction	4.1±0.33	3.8±0.64	4.72±0.40
b_{QRS}-ACT interval in area with transverse conduction	8.7±0.41**	11.9±3.05*,**	11.82±2.01*,**
ARI in area with longitudinal conduction	128±6	146±6*	157±7*
ARI in area with transverse conduction	120±7	142±8*	147±7*

*P<0.05 Significant differences vs. young hearts
**P<0.05 Significant differences between longitudinal and transverse

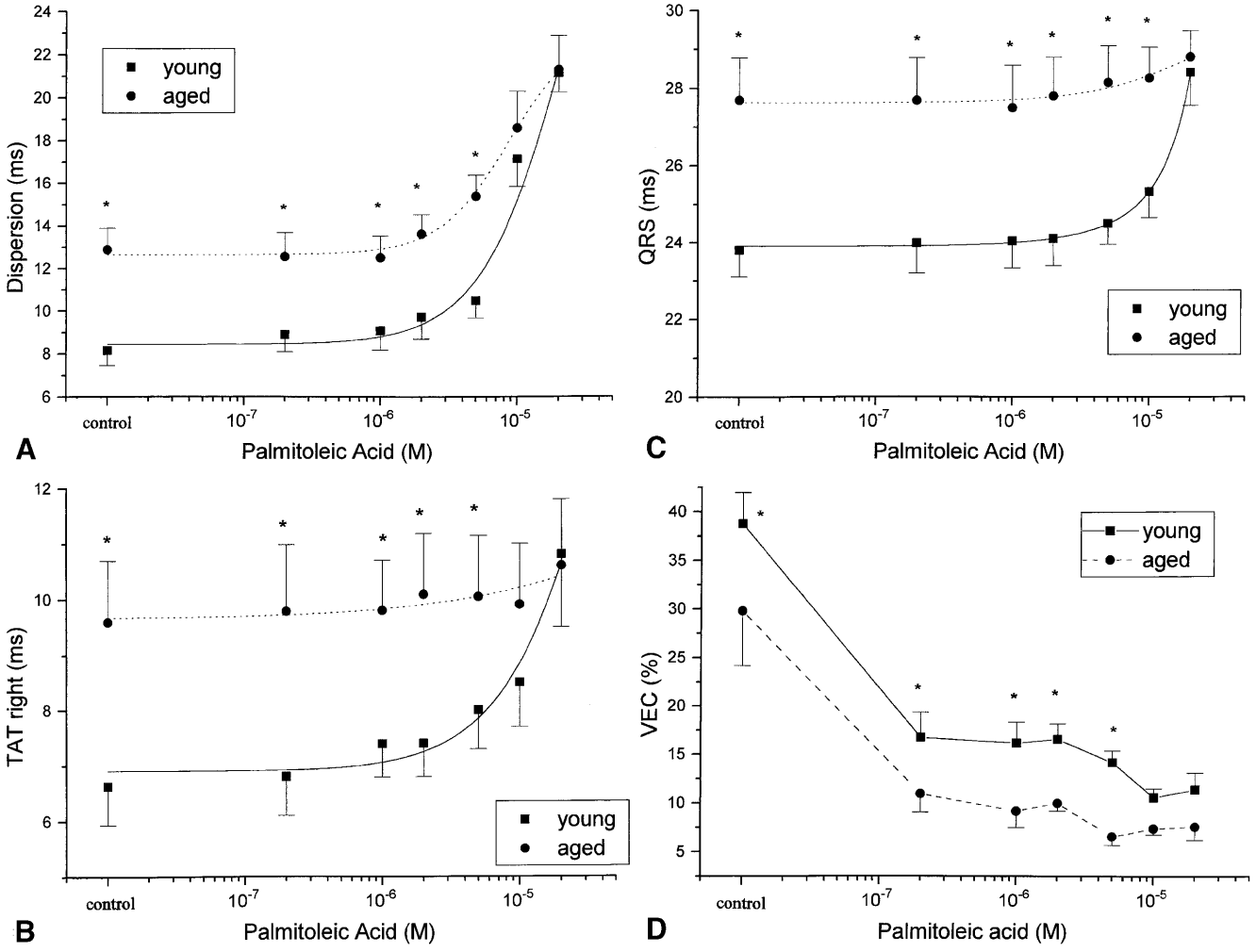

Fig. 4 Concentration-response curves for the effect of palmitoleic acid on dispersion of epicardial activation-recovery intervals (dispersion = standard deviation of the activation-recovery intervals at 256 electrodes; **A**), on the total activation time at the right ventricle (*TAT right*; **B**), on the duration of the QRS complexes (*QRS*; **C**) and on the similarity of the vector fields, expressed as the percentage of vectors with similar direction (if two heart beats are compared; **D**) in young (n=7) and aged rabbit hearts (n=7). Data are given as means ± SEM. *P<0.05 Significant differences between both groups

with 1:1 transmission in young hearts. In aged hearts similar values for the atrioventricular conduction time were reached as in young hearts under the influence of palmitoelic acid: starting at 45±3 ms (young) or 49±4 ms (aged) palmitoleic acid at the highest concentration led to a significantly prolonged *PQ* of 58±3 ms (young) or 61±3 ms (aged), the difference between both groups being not significant.

Anisotropy in presence of palmitoleic acid

At the end of the experiments, i.e. under the influence of 20 μM palmitoleic acid, we assessed cardiac anisotropy by application of a brief rectangular pulse. While in young hearts we could elicit a propagated response allowing the calculation of V_L and V_T, in aged hearts, however, it was not possible to elicit a propagated activation by external stimulation under 20 μM palmitoleic acid. In young hearts V_L and V_T were reduced: V_L: from 0.53±0.02 m/s to 0.44±0.04 m/s, P<0.05; V_T: from 0.28±0.02 m/s to 0.21±0.02 m/s, P<0.05), i.e. the percentage change in V_T (–25±5%) was somewhat higher than that in V_L (–17±6%). Anisotropic ratio, thus, was slightly enhanced from 1.89±0.1 to 2.12±0.1 (P=0.12). The time interval between the beginning of the QRS complex and the activation time point at that certain electrode (b_{QRS}-ACT) was prolonged by palmitoleic acid predominantly and significantly in areas with transverse conduction (Table 1).

Histological findings; cell capacitance

We found in classical H&E and Van Gieson-stained slices an increased amount of connective tissue with deposition of collagen in aged hearts (Fig. 5). It became obvious that broad collagen strands were found lateral of the cells thereby separating the fibers. Planimetric analysis of 10,000 μm^2 revealed a percentage of 18±6% connective tissue in aged vs. 2±1% in young hearts. Cell capacitance

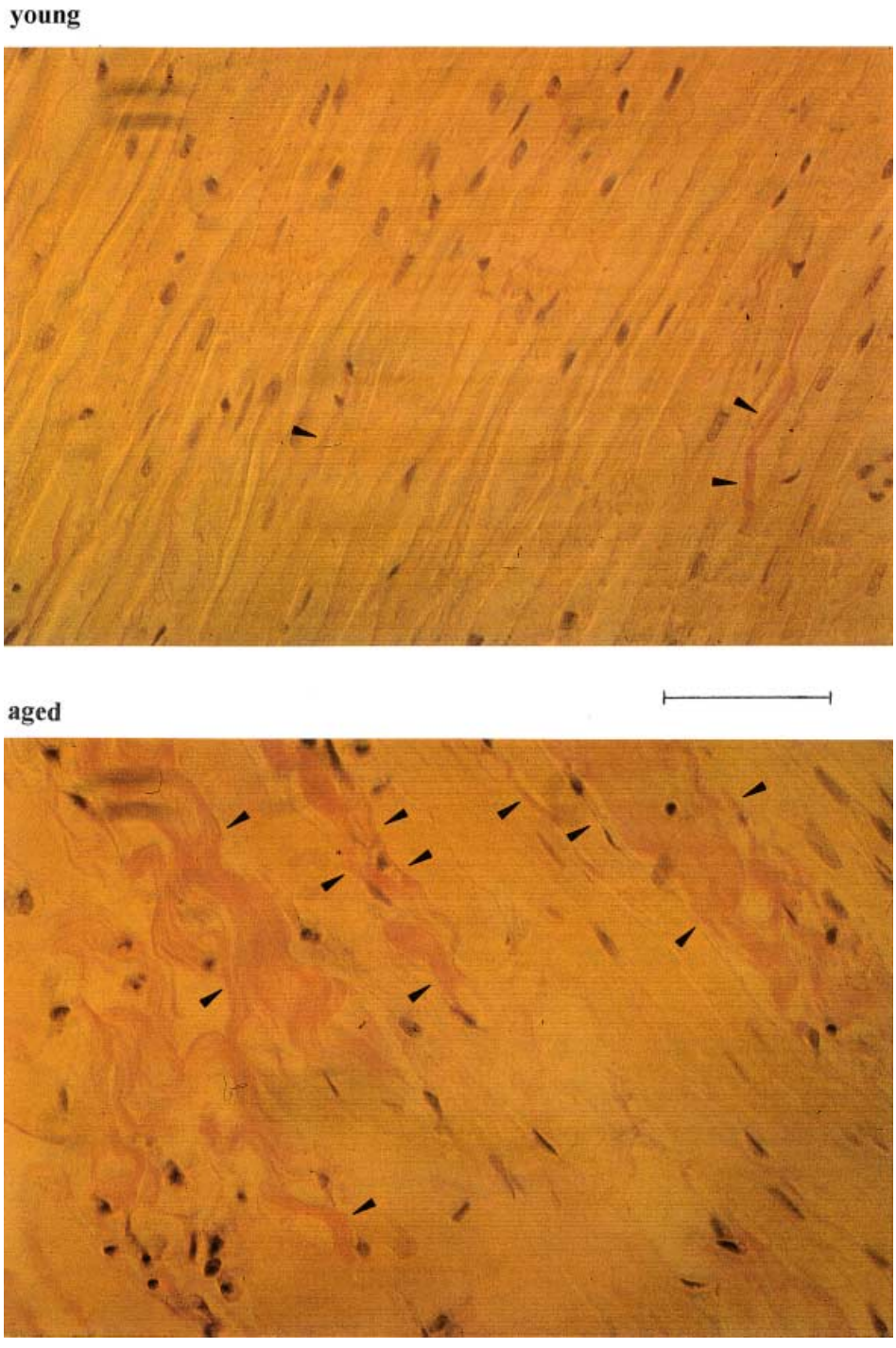

Fig. 5 Van Gieson-stained slice of the left ventricular tissue of a young (*upper panel*) and of an aged rabbit heart (*lower panel*), ×400. Note the light red-stained collagenous connective tissue (indicated by the *triangles*). Both photographs were taken at the same magnification (×400). The *bar* indicates 100 μM

was increased from 106±37 pF (young) to 265±97 pF (aged), i.e. increase by a factor of 2.5±0.2, indicating increased cell size.

Regarding the distribution of Cx43 in the ventricles we found the typical distribution of Cx43 in young hearts with accentuated immunofluorescence at the cell poles, so that 73±8% of the polar membrane length were immunofluorescence-positively stained, while only 4.7±0.8% of the lateral membrane were positively stained. In aged hearts, a larger proportion of the lateral membrane was immunofluorescence positive (10.3±2.4%, $P<0.05$). The proportion of the positively stained polar membrane was also, but not significantly, enhanced (84.5±9%; Fig. 6).

Discussion

Our basic electrophysiological findings in aged hearts, prolonged total activation time, broadened and fractionated QRS complexes, enhanced beat-to-beat variability of

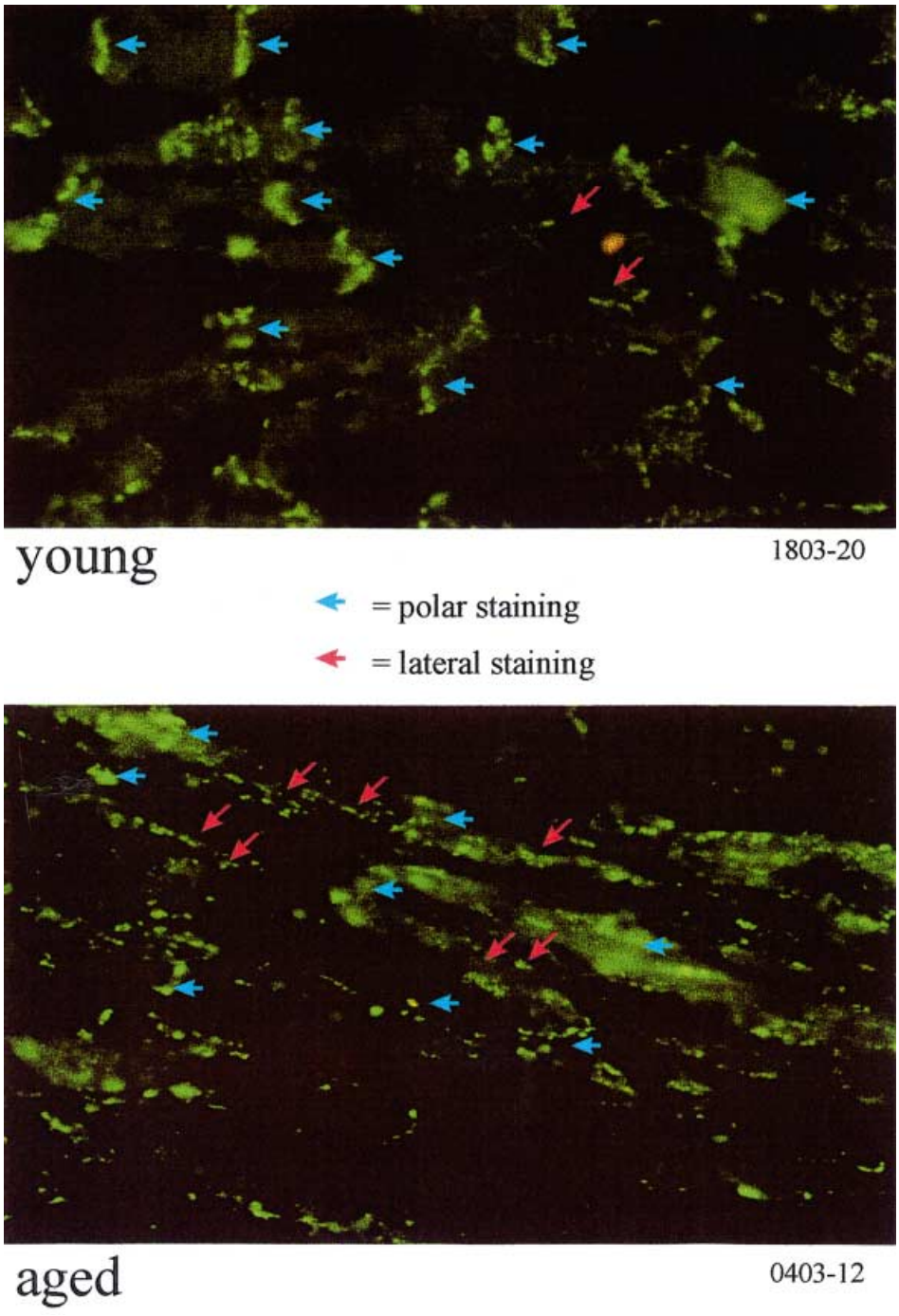

Fig. 6 Cx43 immunostaining of the left ventricular tissue of a young (*upper panel*) and of an aged rabbit heart (*lower panel*). Both photographs were taken at the same magnification (×400). The *bar* indicates 100 μM. Note that the typical tile-like pattern of Cx43 immunofluorescence (with staining at the cell ends) can be seen in young heart, but is more irregular in the aged heart

the activation pattern, slowed transverse conduction (but only slightly affected longitudinal conduction) and increased anisotropy indicate a disturbance of conduction and a change in the biophysical properties of the tissue. Thus, broadened QRS complexes in unipolar epicardial electrograms have been shown to reflect a slowing of the wave under the measuring electrode (Burgess et al. 1988), while fractionated QRS complexes, i.e. multiple peaks in the extracellular waveforms, are caused by inhomogeneities of the local conduction and indicate that propagation is discontinuous (Spach and Dolber 1990) and non-uniform due to side-to-side uncoupling (Spach and Dolber 1986; Spach and Heidlage 1995). Both broadening and fractionation of the QRS complexes were observed in our study in aged hearts and thus may indicate slowing, non-uniformity and discontinuity of conduction. Non-uniform discontinuous propagation can be assumed to lead to a higher beat-to-beat variability (Frame and Simson 1988; Spach and Dolber 1986; Spach et al. 1989a, 1989b). Accordingly, in aged hearts we observed a lower percentage of vectors with similar direction, if two succeeding heart beats are compared, which indicates a higher beat-to-beat

variability of the activation spreading and is compatible with a higher non-uniformity in aged hearts.

In our experiments, predominantly transverse conduction was decreased in aged hearts. Accordingly, one should expect that the time interval between the beginning of the QRS complex and the activation time point (b_{QRS}-ACT interval), as a measure of local conduction (Burgess et al. 1988), should be (a) increased in aged hearts in areas of transverse conduction and (b) longer than that in areas with longitudinal conduction (Burgess et al. 1988; Spach and Dolber 1990). This is shown by the data in our study (Table 1). In addition, a predominant effect on the transverse conduction as seen in our study would mean that – since spreading of activation in the heart is maintained by intercellular contacts via gap junctions – functional side-to-side contacts may be reduced in aged hearts. In support of this hypothesis the histological examination of the hearts in our study revealed that many of the fibers were indeed separated by broad collagen strands lateral to the fibers thus impairing the close side-to-side contact. The finding of lateral deposition of collagen (this study) could explain reduced transverse conduction velocity.

If such a change in the biophysical properties of the tissue occurs, one could expect that inhomogeneities in the repolarization should also occur (Dhein 1998a, 1998b; Spach and Dolber 1986; Spach et al. 1988, 1989a, 1989b). Thus, we investigated the dispersion of activation recovery intervals. Regarding the interpretation of this parameter, the activation time point in unipolar electrograms is coincident with the upstroke of the action potential (Durrer and Van der Tweel 1954), while the repolarization time points measured as $t(dU/dt_{max})$ during the *T*-wave are coincident with the repolarisation of the action potential (Burgess et al. 1988; Franz 1993; Millar et al. 1985). Thus, ARI in unipolar extracellular electrograms (as in this study) is not equal but is an indicator of local action potential duration. Moreover, it has been shown that ARI correlates very well with the local effective refractory period (r=0.97; Millar et al. 1985).

Our results indicated a significant prolongation of ARI at right and back wall in aged hearts. This is in good accordance with findings of Cerbai and coworkers (1994) describing prolonged action potentials in aged rats caused by decreased presence of the repolarizing potassium current $I_{t.o.}$, while I_{K1} was not affected. The dispersion of ARI, i.e. standard deviation of ARI at 256 sites, is an indicator of the degree of inhomogeneity of repolarisation. An increase in dispersion can be attributed to either reduced gap junctional coupling (Lesh et al. 1989; Müller and Dhein 1993), to inhomogeneities in the expression of repolarizing currents (Antzelevitch et al. 1996; Sicouri et al. 1997) or to local ischemia (Gottwald et al. 1998; Kléber et al. 1978; Kuo et al. 1983). In freshly isolated cells intrinsic action potential duration of cardiomyocytes is known to exhibit some variability. If in tissue two adjacent cells develop action potentials of different duration, i.e. repolarizing at different time points, this will produce a gradient in potential between both cells, which normally is compensated for by a current flowing from one cell to the other via the intercellular gap junction channels. Viceversa, uncoupling can enhance or unmask such differences and can result in an increase in dispersion (Lesh et al. 1989). According to common theory (e.g. Cole et al. 1988), enhanced dispersion is due to the fact that differences in action potential duration generating potential differences can not or only partially be equalized by compensatory currents if coupling is reduced (Cole et al. 1988). In line with this, we found slightly longer ARI in areas of longitudinal conduction than in areas of transverse conduction (see Table 1), which may be explained by the hypothesis that in areas with longitudinal conductions more cells are isopotential and thus, there is only little potential gradient among the cells. In addition, uncoupling with palmitoleic acid slightly prolonged ARI in that setting (Table 1; this can only be observed if directional differences are taken into account and if ventricular stimulation is used as in these data), probably due to smaller loss of current to neighboring cells. The interrelationship of coupling and dispersion was also shown in computer simulation models (Lesh et al. 1989; Müller and Dhein 1993; Rudy and Quan 1987). Increased dispersion in atrial tissue has been shown in elegant studies by Spach and colleagues (Spach and Dolber 1986; Spach et al. 1988, 1989a, 1989b) to be related to lateral collagen deposition leading to decreased side-to-side coupling.

Thus, the alterations seen in aged ventricles (i.e. broadened and fractionated QRS complexes, slowed transverse conduction, enhanced beat-to-beat variability, increased anisotropy, enhanced dispersion) are compatible with the hypothesis of reduced intercellular coupling. Slowed conduction can occur either due to reduced sodium channel availability (Buchanan et al. 1985) or ionic changes (Gettes 1990), or to reduced intercellular coupling (Cole et al. 1988; Dekker et al. 1996; Delmar et al. 1987; Joyner 1982). Reduced sodium channel availability would – on the other hand – exert the opposite effect on anisotropy as observed in our study. It was shown in atrium that blocking sodium channels reduces predominantly longitudinal conduction velocity and, thus, decreases anisotropy (Spach et al. 1987). This has also been shown in ventricular tissue (guinea-pig papillary muscle) in an optical mapping study (with the voltage-sensitive dye di-4-ANEPPS) using flecainide (Dhein et al. 1996). However, studies on this question in the more complex free ventricular wall are still missing. In addition, enhanced anisotropy – in our case due to reduced transverse conduction velocity – has also been observed as a consequence of reduced intercellular coupling (Delmar et al. 1987; Dhein et al. 1999) or resulting from differences in longitudinal and transverse cell-cell coupling (Saffitz et al. 1994, 1995). The predominant decrease in transverse conduction in our study is consistent with the assumption of decreased intercellular coupling as shown by Jongsma and Wilders (2000). They simulated a 40% decrease in gap junction conductivity which resulted in a small decrease of V_L by 11% and a larger reduction in V_T by 27%.

Moreover, in a recent sophisticated experimental and computer simulation study Spach et al. (2000) compared

neonatal and adult ventricular cardiomyocytes showing a non-significant increase in cell-to-cell delay of longitudinal propagation but a significant increase in cell-to-cell delay of transverse propagation in adult vs. neonatal cells. However, in that study the authors also show that with enhanced cell size the transverse cell-to-cell delay also increases and intracellular propagation became more discontinuous. In our study, the cell capacitance was increased thus indicating enhanced cell size (in rabbit cardiomyocytes a capacity/volume ratio of 4.58 pF/pl has been determined by Satoh et al. 1996). Thus, the increase in cell size may also contribute to the changes observed in our study. However, the collagenous strands separating the fibers and impairing close side-to-side contacts also have to be considered.

According to the discussion of Spach and colleagues (2000) the more homogeneous distribution of Cx43 at the lateral cell borders in aged hearts may mitigate to some degree discontinuities evoked by the increased cell size, although from our data it remains unclear whether these Cx43 depositions represent functional channels. In line with the above findings and studies, our data show age-dependent slowing of transverse propagation comparing young and aged rabbits. Taken together, these studies (Delmar et al. 1987; Dhein et al. 1999; Spach and colleagues 2000; and of Jongsma and Wilders 2000 in concert with our data – slowing of transverse conduction and enhanced dispersion) may indicate an age-dependent slowing of conduction in the ventricle which might be caused by a reduction of gap junction coupling.

If so, a gap junction uncoupling agent applied to young hearts should mimic the effects of aging. In support of this view, the experiments using palmitoleic acid (a gap junction blocking agent; Burt et al. 1991; Dhein et al. 1999) indicate that this substance alters the biophysical and electrophysiological properties (e.g. velocities: transverse > longitudinal, anisotropy, QRS, dispersion, activation patterns) in the same way as aging and, furthermore, that at the highest concentration young and aged hearts end up at the same level of a certain parameter. In young hearts experimental reduction in gap junction coupling with palmitoleic acid leads to enhanced dispersion, reduced similarity of activation vectors with similar direction, increased total activation time, indicating slowed conduction, and increased anisotropy due to decreased transverse conduction velocity in good accordance with a previous investigation (Dhein et al. 1999) or with investigations using heptanol as gap junction uncoupling agent (Delmar et al. 1987). The observed effects of palmitoleic acid have been explained as a reduction in intercellular coupling (Burt et al. 1991; Dhein et al. 1999). Interestingly, similarity of vector fields was more sensitive to treatment with palmitoleic acid as became evident from the slightly lower EC_{50} (<0.2 μM) in comparison to EC_{50} values for the other effects (which were in the order of 5–7 μM). Together with the findings reported by Spach et al. (1988, 1989a, 1989b, 2000) and Burgess et al. (1988) it can be argued that even small changes in local conduction will cause large effects on the activation pattern, so that similarity of vector fields can be expected to be very sensitive to changes in intercellular coupling.

Thus, the application of palmitoleic acid mimicked the effects observed in aged hearts. In aged hearts, in principle similar effects of palmitoleic acid were observed in the present study. However, since initial "pre-drug" values for dispersion of ARI or total activation time were higher in aged hearts, concentration-response curves were flat in these hearts, but reached similar maximum values at the highest concentration with similar EC_{50} values. The unsaturated fatty acids like palmitoleic acid, as alcohols such as heptanol, octanol or decanol (Niggli et al. 1989; Rüdisüli and Weingart 1989), are assumed to incorporate into the membrane by a simple physicochemical mechanism (Bastiaanse et al. 1993; Burt et al. 1993), thereby reducing the fluidity of membranous cholesterol-rich domains (Bastiaanse et al. 1993) and increasing the disorder in the interior of the membrane (Burt et al. 1991, 1993; Goldstein 1984; Gruber and Low 1988; Klausner et al. 1980).

Interestingly, application of the gap junction uncoupler palmitoleic acid in young hearts led to the same pattern of conduction slowing so that b_{QRS}-ACT was prolonged in areas with transverse conduction (from 8.77 ms to 11.8 ms) but only slightly affected in areas with longitudinal conduction (4.05 ms vs. 4.72 ms; see Results and Table 1) thus mimicking the effects of aging. Taken together, application of the gap junction uncoupler palmitoleic acid in young hearts leads to very similar alterations of the cardiac electrophysiology (transverse slowing, enhanced anisotropy, QRS broadening, enhanced dispersion of ARI) and thus mimics the changes observed with aging.

In conclusion, propagation becomes inhomogeneous and non-uniform, anisotropy increases and intercellular coupling seems to be reduced in the ventricles of aged hearts, resulting in decreased transverse conduction and enhanced dispersion of ARI.

Acknowledgements The authors thankfully acknowledge the skillful technical assistance of Mrs. Karina Abuazi-Paulus and the financial support by a grant given by the Deutsche Forschungsgemeinschaft DFG (Dh 3/8-1) to S.D.

References

Antzelevitch C, Sun ZQ, Zhang ZQ, Yan GX (1996) Cellular and ionic mechanisms underlying erythromycin-induced long QT intervals and torsade de pointes. J Am Coll Cardiol 28:1836–1848

Bastiaanse EM, Jongsma H, Laarse A van der, Takens-Kwak BR (1993) Heptanol-induced decrease in cardiac gap junctional conductance is mediated by a decrease in the fluidity of membranous cholesterol-rich domains. J Membr Biol 136:135–145

Bazett HC (1920) An analysis of the time relations of electrocardiograms. Heart 7:353–370

Buchanan JW, Saito T, Gettes LS (1985) The effects of antiarrhythmic drugs, stimulation frequency, and potassium-induced resting membrane potential changes on conduction velocity and dV/dt_{max} in guinea pig myocardium. Circ Res 56:696–703

Burgess MJ, Steinhaus BM, Spitzer KW, Ershler PR (1988) Nonuniform epicardial activation and repolarization properties of in-vivo canine pulmonary conus. Circ Res 62:233–246

Burt JM, Massey KD, Minnich BN (1991) Uncoupling of cardiac cells by fatty acids: structure-activity relationships. Am J Physiol 260:C439–C448

Burt JM, Minnich BN, Massey KD, Ovadia M, Moore LK, Hirschi KK (1993) Influence of lipophilic compounds on gap junction channels. In: Hall JE, Zampighi GA, Davies RM (eds) Gap junctions. Progress in cell research, vol 3. Elsevier Science Publishers, Amsterdam, pp 113–120

Cerbai E, Barbieri M, Li Q, Mugelli A (1994) Ionic basis of action potential prolongation of hypertrophied cardiac myocytes isolated from hypertensive rats of different ages. Cardiovasc Res 28:1180–1187

Cole WC, Picone JB, Sperelakis N (1988) Gap junction uncoupling and discontinuous propagation in the heart. Biophys J 53:809–818

Dekker LRC, Fiolet JWT, VanBavel E, Coronel R, Opthof T, Spaan JAE, Janse MJ (1996) Intracellular Ca^{2+}, intercellular electrical coupling and mechanical activity in ischemic rabbit papillary muscle. Effects of preconditioning and metabolic blockade. Circ Res 79:237–246

Delmar M, Michaels DC, Johnson T, Jalife J (1987) Effects of increasing intercellular resistance on transverse and longitudinal propagation in sheep epicardial muscle. Circ Res 60:780–785

Dhein S (1998a) Cardiac gap junctions. Karger, Basel, pp 3–132

Dhein S (1998b) Gap junction channels in the cardiovascular system: pharmacological and physiological modulation. Trends Pharmacol Sci 19:229–241

Dhein S, Rutten P, Klaus W (1988) A new method for analysing the geometry and time course of epicardial potential spreading. Int J Biomed Computing 23:201–207

Dhein S, Müller A, Klaus W (1990) Prearrhythmia: changes preceding arrhythmia, new aspects by epicardial mapping. Basic Res Cardiol 85:285–296

Dhein S, Müller A, Gerwin R, Klaus W (1993) Comparative study on the proarrhythmic effects of some antiarrhythmic agents. Circulation 87:617–630

Dhein S, Hartbauer M, Müller W, Windisch H, Salameh A, Tritthart HA (1996) Flecainide alters the cardiac microscopic activation pattern. An in-vitro study using voltage-sensitive dyes. Pharmacol Res 34:125–130

Dhein S, Krüsemann K, Schaefer T (1999) Effects of the gap junction uncoupler palmitoleic acid on the activation and repolarization wavefronts in isolated rabbit hearts. Br J Pharmacol 128:1375–1384

Durrer D, Van der Tweel LH (1954) Spread of activation in the left ventricular wall of the dog. Activation conditions at the epicardial surface. Am Heart J 47:192–203

Frame LH, Simson MB (1988) Oscillations of conduction, action potential duration and refractoriness. Circulation 78:1277–1287

Franz MR (1993) Monophasic action potential mapping. In: Shenasa M, Borggrefe M, Breithardt G (eds) Cardiac mapping. Futura, Mount Kisco, pp 565–583

Gettes LS (1990) Effects of ionic changes on impulse propagation. In: Rosen MR, Janse MJ, Wit AL (eds) Cardiac electrophysiology. Futura, Mount Kisco, pp 459–480

Gottwald M, Gottwald E, Dhein S (1997) Age-related electrophysiological and histological changes in rabbit hearts. Int J Cardiol 62:97–106

Gottwald E, Gottwald M, Dhein S (1998) Enhanced dispersion of epicardial activation-recovery intervals at sites of histological inhomogeneity during regional cardiac ischaemia and reperfusion. Heart 79:474–480

Gruber HJ, Low PS (1988) Interaction of amphiphiles with integral membrane proteins. I. Structural destabilization of the anion transport protein of the erythrocyte membrane by fatty acids, fatty alcohols and fatty amines. Biochim Biophys Acta 944:414–424

Jongsma HJ, Wilders R (2000) Gap junctions in cardiovascular disease. Circ Res 86:1193–1197

Joyner RW (1982) Effects of the discrete pattern of electrical coupling on propagation through an electrical syncytium. Circ Res 50:192–200

Klausner SC, Schwartz AB (1985) The aging heart. Clin Geriatr Med 1:119–141

Kléber AG, Janse MJ, Capelle FJL van, Durrer D (1978) Mechanism and time course of ST and TQ segment changes during acute regional myocardial ischemia in the pig heart determined by extracellular and intracellular recordings. Circ Res 42:603–613

Kuo CS, Munakata K, Reddy CP, Surawicz B (1983) Characteristics and possible mechanism of ventricular arrhythmia dependent on the dispersion of action potential durations. Circulation 67:1356–1367

Lesh MD, Pring M, Spear JF (1989) Cellular uncoupling can unmask dispersion of action potential duration in ventricular myocardium. Circ Res 65:1426–1440

Millar CK, Kralios FA, Lux RL (1985) Correlation between refractory periods and activation recovery intervals from electrograms: effects of rate and adrenergic interventions. Circulation 72:1372–1379

Müller A, Dhein S (1993) Sodium channel blockade enhances dispersion of the cardiac action potential duration. A computer simulation study. Basic Res Cardiol 88:11–15

Müller A, Dhein S, Klaus W (1991) Heterogeneously distributed sensitivities to potassium as a cause of hypokalemic arrhythmias in isolated rabbit hearts. J Cardiovasc Electrophysiol 2:145–155

Niggli E, Rüsisüli A, Maurer P, Weingart R (1989) Effects of general anaesthetics on current flow across junctional and nonjunctional membranes and contractility in guinea pig myocytes. Am J Physiol 256:C273–C281

Rüdisüli A, Weingart R (1989) Electrical properties of gap junction channels in guinea pig ventricular cell pairs revealed by exposure to heptanol. Pflugers Arch 415:12–21

Rudy Y, Quan WL (1987) A model study of the effects of the discrete cellular structure on electrical propagation in cardiac tissue. Circ Res 61:815–823

Saffitz JE, Kanter HL, Green KG, Tolley TK, Beyer EC (1994) Tissue specific determinants of anisotropic conduction velocity in canine atrial and ventricular myocardium. Circ Res 74: 1065–1070

Saffitz JE, Davis LM, Darrow BJ, Kanter HL, Laing JG, Beyer EC (1995) The molecular basis of anisotropy: role of gap junctions. J Cardiovasc Electrophysiol 6:498–510

Satoh H, Delbridge LMD, Blatter LA, Bers DM (1996) Surface: volume relationship in cardiac myocytes studied with confocal microscopy and membrane capacitance measurements: species-dependence and developmental effects. Biophys J 70:1494–1504

Sicouri S, Moro S, Litovsky S, Elizari MV, Antzelevitch C (1997) Chronic amiodarone reduces transmural dispersion of repolarization in the canine heart. J Cardiovasc Electrophysiol 8: 1269–1279

Spach MS, Dolber PC (1986) Relating extracellular potentials and their derivatives to anisotropic propagation at a microscopic level in human cardiac muscle. Circ Res 58:356–371

Spach MS, Dolber PC (1990) Discontinuous anisotropic propagation. In: Rosen MR, Janse MJ, Wit AL (eds) Cardiac electrophysiology. A textbook. Futura, Mount Kisco, pp 517–534

Spach MS, Heidlage JF (1995) The stochastic nature of cardiac propagation at a microscopic level. Electrical description of myocardial architecture and its application to conduction. Circ Res 76:366–380

Spach MS, Dolber PC, Heidlage JF, Kootsey JM, Johnson EA (1987) Propagating depolarization in anisotropic human and canine cardiac muscle: apparent directional differences in membrane capacitance. Circ Res 60:206–219

Spach MS, Dolber PC, Heidlage JF (1988) Influence of the passive anisotropic properties on directional differences in propagation following modification of the sodium conductance in human atrial muscle. A model of reentry based on anisotropic discontinuous propagation. Circ Res 62:811–832

Spach MS, Dolber PC, Heidlage JF (1989a) Interaction of inhomogeneities of repolarization with anisotropic propagation in dog atria. Circ Res 65:1612–1631

Spach MS, Dolber PC, Anderson PAW (1989b) Multiple regional differences in cellular properties that regulate repolarization and contraction in the right atrium of adult and newborn dogs. Circ Res 65:1594–1611

Spach MS, Heidlage JF, Dolber PC, Barr RC (2000) Electrophysiological effects of remodeling cardiac gap junctions and cell size. Circ Res 86:302–311